



*J. Serb. Chem. Soc.* 77 (1) 53–66 (2012)  
JSCS–4248

## Spectroscopic properties and antimicrobial activity of dioxomolybdenum(VI) complexes with heterocyclic *S,S'*-ligands

SOFIJA P. SOVILJ<sup>1\*#</sup>, DRAGANA MITIĆ<sup>1#</sup>, BRANKO J. DRAKULIĆ<sup>2</sup>  
and MARINA MILENKOVIĆ<sup>3</sup>

<sup>1</sup>Faculty of Chemistry, P. O. Box 118, 11158 Belgrade, Serbia, <sup>2</sup>ICTM, Department of Chemistry, Njegoševa 12, 11001 Belgrade, Serbia and <sup>3</sup>Department of Microbiology and Immunology, Faculty of Pharmacy, University of Belgrade, Vojvode Stepe 450, Belgrade, Serbia

(Received 28 March, revised 26 August 2011)

**Abstract:** Five new dioxomolybdenum(VI) complexes of the general formula  $[\text{MoO}_2(\text{Rdtc})_2]$ , **1–5**, where Rdtc<sup>−</sup> refer to piperidine (Pipdtc), 4-morpholine (Morphdtc), 4-thiomorpholine (Timdtc), piperazine (Pzdtc) or *N*-methylpiperazine (*N*-Mepzdtc) dithiocarbamates, respectively, have been prepared. The complexes were characterized by elemental analysis, conductometric measurements, electronic, IR and NMR spectroscopy. The complexes **1–5** contain a *cis*-MoO<sub>2</sub> group and have an octahedral geometry. Two dithiocarbamate ions join as bidentates with both the sulfur atoms to the molybdenum atom. The presence of different heteroatoms in the piperidino moiety influences the  $\nu(\text{C}=\text{N})$  and  $\nu(\text{C}=\text{S})$  vibrations, which wavelengths decrease in the order: Pipdtc > *N*-Mepzdtc > Morphdtc > Pzdtc > Timdtc ligands. Based on their spectral data, the molecular structures of complexes **1–5** were optimized at the semi-empirical molecular-orbital level, and the geometries, as obtained from calculations, are described. The antimicrobial activities of the complexes were tested against nine different laboratory control strains of bacteria and two strains of the yeast *Candida albicans*. All the tested strains were sensitive. Complexes bearing heteroatom in position 4 of piperidine moiety were significantly more potent against the tested bacteria compared to the corresponding ligands.

**Keywords:** dithiocarbamates; molybdenum(VI) complexes; MoO<sub>2</sub><sup>2+</sup> group; geometry optimization.

### INTRODUCTION

Molybdenum complexes with organic ligands are compounds of great theoretical and practical interest, especially valuable as model systems for biochemi-

\* Corresponding author. E-mail: ssovilj@chem.bg.ac.rs

# Serbian Chemical Society member.

doi: 10.2298/JSC110328160S

cal processes. The presence of  $[\text{Mo}^{\text{VI}}\text{O}_2]^{2+}$  groups can serve as oxygen atom transfer agents and is of importance in the fully oxidized states of a number of redox enzymes, in which their active site consists of a *cis*-molybdenum dioxo moiety.<sup>1,2</sup> In recent years, their antimicrobial potency has gained special attention against both human and plant pathogenic microorganisms.<sup>3,4</sup>

Moreover, dithiocarbamato ( $\text{Rdtc}^-$ ) ligands are known to form stable complexes with many transition metals.<sup>5–14</sup> Interest in dithiocarbamate complexes arises because of their versatile structures, depending on the manner of coordination,<sup>15–19</sup> and the type of their biological activity.<sup>20–24</sup> Additionally, these coordination compounds have intriguing properties, being good corrosion inhibitors in acidic media.<sup>23–27</sup>

The aim of the present study was to synthesize dioxomolybdenum(VI) complexes with piperidine- ( $\text{Pipdtc}$ ), 4-morpholine- ( $\text{Morphdtc}$ ), 4-thiomorpholine- ( $\text{Timdtc}$ ), piperazine- ( $\text{Pzdtc}$ ) and *N*-methylpiperazine- ( $\text{N-Mepzdtc}$ ) dithiocarbamato ligands. As a contribution to the problem of the coordination behavior of heteroalicyclic dithiocarbamates, their mode of coordination was determined and, particularly, the spectrochemical properties of these compounds are discussed. In order to obtain further insight of the electronic structure of the complexes, the effect of heteroatom variation in the piperidino moiety on the C–N, and the C–S bonds, as well as on the electronic structure of the complexes was examined. Molecular modeling is a powerful tool to add chemical and physical information to the information obtained by other techniques.<sup>28–32</sup> For these reasons, based on the available spectral data, the molecular structures of all the prepared complexes, **1–5**, was optimized and a description of the structural parameters is given. Finally, the complexes were examined as potential antimicrobial agents.

## EXPERIMENTAL

### *Syntheses of the $[\text{MoO}_2(\text{Rdtc})_2]$ complexes 1–5*

All the used chemicals were commercial products of analytical reagent grade. The starting acetylacetonato complex  $[\text{MoO}_2(\text{acac})_2]$  and the sodium salts of  $\text{Rdtc}^-$  were prepared as described in the literature.<sup>12,33</sup>

To a methanolic solution ( $5 \text{ cm}^3$ ) of  $\text{MoO}_2(\text{acac})_2$  (330 mg, 1.0 mmol) was added dropwise 2.0 mmol of the corresponding  $\text{NaRdtc} \cdot 2\text{H}_2\text{O}$  ligand (*i.e.*, 468 mg of  $\text{Pipdtc}$ ; 452 mg of  $\text{Morphdtc}$ ; 484 mg of  $\text{Timdtc}$ ; 450 mg of  $\text{Pzdtc}$  or 478 mg of  $\text{N-Mepzdtc}$ ) dissolved in water ( $5 \text{ cm}^3$ ), during 1 h under stirring and thermostating at  $40 \text{ }^\circ\text{C}$ . The mixture was then continuously stirred under reflux for about 2 h. The filtrate was concentrated under vacuum to  $10 \text{ cm}^3$ . Upon cooling the mixture for two days in a refrigerator, the crude products precipitated. After recrystallization from a 1-heptene/toluene mixture (1:1, v/v), light brown crystalline substances of the corresponding complexes were obtained.

### *Materials and methods*

Elemental analyses (C, H, N) were performed by standard micro methods at the Department of Instrumental Analyses of the Institute of Chemistry, Technology and Metallurgy (ICTM), Belgrade. The molar conductivity of methanolic solutions ( $1.0 \times 10^{-3} \text{ mol dm}^{-3}$ ) was

measured at 20 °C using a Jenway-4009 conductometer. The electronic spectra of methanol solutions ( $1.0 \times 10^{-3}$  M) were recorded on a GBC UV/VIS 911 A spectrophotometer. The IR spectra in the 4000–400  $\text{cm}^{-1}$  ranges were measured on a Perkin Elmer 31725x FTIR spectrophotometer, using KBr discs. The  $^1\text{H}$ - and  $^{13}\text{C}$ -NMR spectra were taken on a Varian Gemini 200 instrument at 200/50 MHz in  $\text{DMSO-}d_6$ , at room temperature. All chemical shifts are reported in ppm downfield from tetramethylsilane (TMS), used as the internal standard.

Molecular modeling was realized by MOPAC2009,<sup>34</sup> a general-purpose semi-empirical molecular orbital package for the study of the solid state and molecular structures. The semi-empirical molecular-orbital (MO) PM6 method<sup>35</sup> was used. Geometry optimizations (full optimization of bond angles and bond distances), without any input constraints, were performed by Eigenvector following optimization with a convergence limit of  $0.001 \text{ kcal mol}^{-1} \text{ \AA}^{-1}$ . Geometry optimization of the complexes **1–5** were realized in vacuum and by using implicit solvation in water (COSMO).<sup>36</sup> The IR spectra of the representative complex **1** was obtained from the initial structure assessed by the semi-empirical MO PM6 method additionally optimized on the DFT level (B3LYP) using the LanL2DZ basis set, without any constraint. The  $^1\text{H}$ - and  $^{13}\text{C}$ -NMR spectra were calculated by the Gauge-Independent Atomic Orbital (GIAO) method,<sup>37</sup> using single point calculation (B3LYP/LanL2DZ) and implicit solvation in dimethyl sulfoxide (PCM)<sup>38</sup> on the structure assessed by the semi-empirical MO PM6 method. All calculations on the DFT level were realized by the Gaussian03 suit of programs.<sup>39</sup> Superimposition of the calculated structures for complexes **1** and **3** with the experimentally obtained crystal structures of similar ones taken from literature was realized by VegaZZ 2.4.0.<sup>40</sup> The complexes and their molecular orbitals were visualized by Jmol.<sup>41</sup> All computations were performed on AMD Athlon 64 x2 Dual Core Processors, in Windows or Linux environments.

#### Antimicrobial activity

The antimicrobial activities of the synthesized complexes were evaluated using nine laboratory control strains of bacteria, *i.e.*, the Gram-positive: *Staphylococcus aureus* (ATCC 25923), *S. epidermidis* (ATCC 12228), *Micrococcus luteus* (ATCC 9341), *M. flavus* (10240), *Enterococcus faecalis* (ATCC 29212), *Bacillus subtilis* (ATCC 6633) and the Gram-negative: *Escherichia coli* (ATCC 25922), *Klebsiella pneumoniae* (NCIMB 9111), *Pseudomonas aeruginosa* (ATCC 27853), and two strains of yeast, *i.e.*, *Candida albicans* (ATCC 24433 and ATCC 10259). The microorganisms were provided by the Institute for Immunology and Virology, Torlak, Belgrade, Serbia. A broth microdilution method was used to determine the minimal inhibitory concentration (MIC) of complexes **1–5**, according to the Clinical and Laboratory Standards Institute (CLSI 2005).

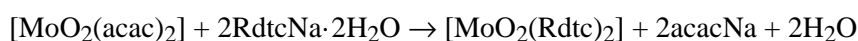
All tests were performed in Müller Hinton broth for the bacterial strains and in Sabouraud dextrose broth for the yeasts. Overnight broth cultures of each strain were prepared, and the final concentration in each well was adjusted to  $2 \times 10^6$  CFU  $\text{ml}^{-1}$  for the bacteria and  $2 \times 10^5$  CFU  $\text{ml}^{-1}$  for the yeasts. The investigated compounds were dissolved in 1 % dimethyl sulfoxide (DMSO) and then diluted to the highest concentration. Serial doubling dilutions of the compounds were prepared in a 96-well microtiter plate over the concentration range 31.25–1000  $\mu\text{g ml}^{-1}$ . In the tests, triphenyl tetrazolium chloride (TTC) (Aldrich Chemical Company Inc., USA) was also added to the culture medium as a growth indicator. The final concentration of TTC after inoculation was 0.05 %. The microbial growth was determined from the absorbance at 600 nm, using a universal microplate reader after 24 h incubation at 37 °C for the bacteria and after 48 h incubation at 25 °C for the fungi. The MIC is defined as the lowest concentration of the compound at which no visible growth of microorganism is observed. All determinations were performed in duplicate and two positive growth controls were

included.<sup>42</sup> To resolve structure–activity trends, the *MIC* values of complexes **1–5**, the corresponding ligands and  $[\text{MoO}_2(\text{acac})_2]$  used for comparison, originally determined in mass concentration ( $\mu\text{g ml}^{-1}$ ), were converted to molar concentrations (M).

## RESULTS AND DISCUSSION

### *Syntheses and physico–chemical properties of the complexes*

Complexes **1–5** were obtained by mixing the reactants in a 1:2 molar ratio, in a substitution reaction of the two acetylacetonato anions in the  $[\text{MoO}_2(\text{acac})_2]$  complex by  $\text{Rdtc}^-$  ligands:



The obtained complexes were light brown microcrystalline substances, stable under atmospheric conditions and soluble in methanol, ethanol, 1-heptene, toluene and dimethyl sulfoxide and insoluble in water, chloroform, dichloromethane and benzene.

The analytical results confirmed the proposed composition:

$[\text{MoO}_2(\text{Pipdtc})_2]$  (**1**). Yield: 106 mg (17 %); Anal. Calcd. for  $\text{C}_{12}\text{H}_{20}\text{MoN}_2\text{O}_2\text{S}_4$  (FW: 448.30): C, 32.14; H, 4.49; N, 6.25 %. Found: C, 32.31; H, 4.80; N, 6.38 %;

$[\text{MoO}_2(\text{Morphdtc})_2]$  (**2**). Yield: 90 mg (19.8 %); Anal. Calcd. for  $\text{C}_{10}\text{H}_{16}\text{MoN}_2\text{O}_4\text{S}_4$  (FW: 452.05): C, 26.55; H, 3.57; N, 6.19 %. Found: C, 27.02; H, 4.11; N, 6.20 %;

$[\text{MoO}_2(\text{Timdtc})_2]$  (**3**). Yield: 52 mg (10.8 %); Anal. Calcd. for  $\text{C}_{10}\text{H}_{16}\text{MoN}_2\text{O}_2\text{S}_6$  (FW: 484.05): C, 24.79; H, 4.33; N, 5.79 %. Found: C, 24.44; H, 4.17; N, 5.80 %;

$[\text{MoO}_2(\text{Pzdtc})_2]$  (**4**). Yield: 153 mg (33.8 %); Anal. Calcd. for  $\text{C}_{10}\text{H}_{18}\text{MoN}_4\text{O}_2\text{S}_4$  (FW: 450.08): C, 26.66; H, 4.03; N, 12.45 %. Found: C, 26.39; H, 4.31; N, 11.54 %;

$[\text{MoO}_2(\text{N-Mepzdtc})_2]$  (**5**). Yield: 130 mg (27.1 %); Anal. Calcd. for  $\text{C}_{12}\text{H}_{22}\text{MoN}_4\text{O}_2\text{S}_4$  (FW: 478.10): C, 35.12; H, 4.64; N, 11.71 %. Found: C, 35.37; H, 4.77; N, 11.77 %.

The non-electrolyte nature of the complexes was confirmed by their low molar conductivities<sup>43</sup> ( $\lambda_{\text{M}} = 45.30; 17.80; 25.90; 33.30$  and  $13.70 \Omega^{-1} \text{ cm}^2 \text{ mol}^{-1}$  for complexes **1–5**, respectively).

### *Spectroscopic properties*

*Electronic absorption spectra.* The complexes are diamagnetic, as expected for the  $4d^0$  configuration. Since there are no d electrons, splitting from d–d transitions was not discernible. The absorptions appearing in the electronic spectra in the range of 280–400 nm arise from charge transfer and intraligand transitions, especially due to the  $\text{NCS}_2$  chromophore, but the assignments of charge-transfer spectra are controversial.<sup>44</sup>

*IR Spectra.* The pertinent IR data, *i.e.*,  $\nu(\text{C-N})$ ,  $\nu(\text{C-S})$  vibrations of the free and coordinated  $\text{Rdtc}^-$  ligands,  $\nu(\text{Mo-S})$  bands, as well as the  $\text{MoO}_2^{2+}$  core vibrations of the complexes **1–5** are collected in Table I.

TABLE I. IR spectral data ( $\text{cm}^{-1}$ ) for complexes **1–5**, and for the  $\text{Rdtc}^-$  ligands (abbreviations: *vs*, very strong; *s*, strong; *m*, medium; *w*, weak)

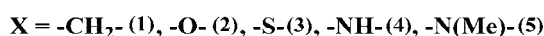
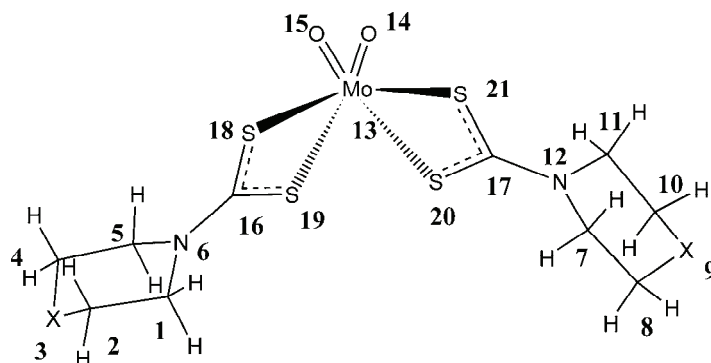
Compound	$\nu(\text{C}\equiv\text{N})$	$\nu(\text{C}\equiv\text{S})$	$\nu(\text{Mo-S})$	$\nu_s(\text{Mo=O})$	$\nu_{as}(\text{Mo=S})$
<b>1</b>	1442 <sub>s</sub>	948 <sub>s</sub>	437 <sub>m</sub>	880 <sub>m</sub>	907 <sub>m</sub>
<b>2</b>	1455 <sub>s</sub>	985 <sub>s</sub>	429 <sub>m</sub>	870 <sub>s</sub>	897 <sub>s</sub>
<b>3</b>	1465 <sub>s</sub>	997 <sub>s</sub>	436 <sub>m</sub>	815 <sub>m</sub>	948 <sub>s</sub>
<b>4</b>	1458 <sub>s</sub>	986 <sub>s</sub>	439 <sub>w</sub>	875 <sub>w</sub>	899 <sub>m</sub>
<b>5</b>	1448 <sub>s</sub>	975 <sub>s</sub>	430 <sub>w</sub>	860 <sub>m</sub>	908 <sub>s</sub>
PipdtcNa	1465 <sub>vs</sub>	965 <sub>s</sub>	–	–	–
MorphdtcNa	1449 <sub>vs</sub>	990 <sub>s</sub>	–	–	–
TimdtcNa	1465 <sub>vs</sub>	995 <sub>s</sub>	–	–	–
PzdtcNa	1460 <sub>vs</sub>	1000 <sub>s</sub>	–	–	–
<i>N</i> -MepzdtcNa	1450 <sub>vs</sub>	995 <sub>s</sub>	–	–	–

Concerning the electronic and structural characteristics of the described compounds, there are several regions of considerable interest in the IR spectra. The 1390–1430  $\text{cm}^{-1}$  region is associated primarily with the thioureide vibration and is attributed to the  $\nu(\text{C}\equiv\text{N})$  vibrations of the  $\text{S}_2\text{C}\equiv\text{NR}_2$  bond<sup>12,14</sup> (Table I). This indicates a significant increase in double bond character of the  $\text{C}\equiv\text{N}$  bond, resulting in higher frequencies compared with the free  $\text{Rdtc}^-$  ligands. All the complexes exhibit  $\nu(\text{C}\equiv\text{N})$  bands in the 1470–1480  $\text{cm}^{-1}$  range, which lie between  $\nu(\text{C=N})$  and  $\nu(\text{C-N})$ , in the 1640–1690 and 1250–1350  $\text{cm}^{-1}$  range,<sup>9</sup> respectively. The 950–1100  $\text{cm}^{-1}$  region is associated with  $\nu(\text{CSS})$  vibrations and has been effectively used to differentiate between monodentate and bidentate  $\text{Rdtc}^-$  ligands.<sup>9,14</sup> In the IR spectra of the obtained complexes, the presence of only one strong band in this region supports a symmetrical bidentate coordination of the dithio ligands, while a doublet expected in the case of monodentate coordination<sup>9</sup> was absent. New absorption bands in the 420–440  $\text{cm}^{-1}$  region, absent in the spectra of the free  $\text{Rdtc}^-$  ligands, are in good agreement with the available literature data.<sup>10,14</sup> The heteroatoms (N, O, S) in the piperidino moiety influence both the  $\nu(\text{C}\equiv\text{N})$  and  $\nu(\text{C}\equiv\text{S})$  values that increase in the order of the complexes with: Pipdtc > *N*-Mepzdtc > Morphdtc > Pzdtc > Timdtc ligands (Table I). This band, however, demonstrates the partial double bond character of the  $\text{C}\equiv\text{S}$  bond on consideration of its position between  $\nu(\text{C=S})$  (1080–1200  $\text{cm}^{-1}$ ) and the  $\nu(\text{C-S})$  bond (600–800  $\text{cm}^{-1}$ ). This behavior can be attributed to the electron releasing ability of the heterocyclic atom that forces a high electron density towards the SCS group.<sup>45,46</sup> The symmetric and antisymmetric stretching vibrations observed near 900  $\text{cm}^{-1}$  can be attributed to a *cis*- $[\text{MoO}_2]^{2+}$  core.<sup>47</sup> Generally, the wave

numbers of  $\nu_{\text{sym}}(\text{Mo}=\text{O})$  vibrations are higher than those of  $\nu_{\text{asym}}(\text{Mo}=\text{O})$ .<sup>48,49</sup> Finally, the skeletal pyperidine bands are located at *ca.* 1610  $\text{cm}^{-1}$ .

The recorded and calculated (see Experimental) IR spectra of complex **1** are shown in Fig. S1 in the Supplementary material. Fair agreement can be visually observed.

*NMR spectra.* Although molybdenum(VI) complexes were well characterized in the solid state, their characterization in solution is necessary in order to evaluate the stability of the obtained complexes under biologically relevant conditions. However, the poor solubility of the molybdenum(VI) complexes **1–5** and the related free ligands hampered NMR experiments in an aqueous environment; therefore, the spectra were recorded in  $\text{DMSO-}d_6$ . The structure enumeration for the structure–spectra assignments are as given in Scheme 1.



Scheme 1. Numbering of the non-hydrogen atoms that correspond to the labels in Table II.

TABLE II.  $^1\text{H}$ - and  $^{13}\text{C}$ -NMR chemical shifts for complexes **1–5** in ppm downfield from TMS. Assignment of the atoms given according to the Scheme 1

Complex	$\delta^1\text{H}$	$\delta^{13}\text{C}$	$\delta^{13}\text{C}$
<b>1</b>	2.51 (2H, <i>t</i> (C1)); 1.91 (2H, <i>s</i> (C2)); 1.68 (2H, <i>s</i> (C3)); 2.00 (2H, <i>s</i> (C4)); 3.36 (2H, <i>s</i> (C5))	$\text{S}_2\text{CN}$ , 190.91	C1(C5), 52.35; C2, 22.13; C3, 25.97; C4, 23.54
<b>2</b>	2.73 (2H, <i>s</i> (C1)); 3.51 (2H, <i>m</i> (C2)); 3.67 (2H, <i>s</i> (C4)); 3.17 (2H, <i>s</i> (C5))	$\text{S}_2\text{CN}$ , 195.42	C1(C5), 51.82; C2, 66.5; C4, 66.5
<b>3</b>	3.27 (2H, <i>t</i> (C1)); 2.58 (2H, <i>s</i> (C2)); 2.82 (2H, <i>m</i> (C4)); 3.27 (2H, <i>t</i> (C5))	$\text{S}_2\text{CN}$ , 201.66	C1(C5), 53.88; C2, 29.54; C4, 29.54
<b>4</b>	2.92 (2H, <i>s</i> (C1)); 2.51 (2H, <i>t</i> (C2)); 1.91 (H, <i>s</i> (C3)); 2.46 (2H, <i>s</i> (C4)); 2.99 (2H, <i>s</i> (C5))	$\text{S}_2\text{CN}$ , 201.93	C1(C5), 66.42; C2, 45.43; C4, 45.43
<b>5</b>	3.39 (2H, <i>s</i> (C1)); 2.51 (2H, <i>d</i> (C2)); 2.25 (3H, <i>t</i> (C3)); 2.40 (2H, <i>s</i> (C4)); 3.39 (2H, <i>s</i> (C5))	$\text{S}_2\text{CN}$ , 197.40	C1(C5), 49.13; C2, 54.96; C4, 54.96; C6, 45.71

The absence of S–H protons and a slight downfield shift of the protons in the NMR spectra of all complexes, with respect to the corresponding ligands, were observed. This indicates that the ligands are coordinated to molybdenum through sulfur atoms.<sup>50</sup> In the <sup>1</sup>H-NMR spectra (Table II), signals of five protons, which belong to the Rdtc<sup>−</sup> ligand, were found for complex **1**. The position and multiplicity of the proton signals for complexes **2–5** depend on the type of heteroatom in position four of the piperidinyli moiety. In the <sup>13</sup>C-NMR spectrum for complex **1**, there are signals at 52.35, 22.13, 25.97 and 23.64 ppm that belong to the Rdtc<sup>−</sup> ligand (Table II). Two signals for complexes **2**, **3** and **4** originated from the symmetrical Rdtc<sup>−</sup> ligands. The last signal, C6, in the spectrum of complex **5** is ascribed to the methyl carbon *N*-Me of *N*-methylpiperidine. Only one signal that corresponds to the CS<sub>2</sub> moieties of Rdtc<sup>−</sup> was observed in the spectrum of each complex, indicating that the chemical environments of the CS<sub>2</sub> moieties of the two Rdtc<sup>−</sup> ligands bound to the *cis*-MoO<sub>2</sub> center are equivalent to each other.<sup>51,52</sup> The experimentally obtained <sup>1</sup>H- and <sup>13</sup>C-NMR spectra for complex **1** and the Pipdtc ligand, and the calculated NMR spectra for complex **1** are given in the Supplementary material. Fair agreement between the calculated and experimentally obtained spectra can be seen (Figs. S2–S4 in the Supplementary material).

#### Molecular modeling

Data of the total energy and heat of formation for each system, as well as selected bond distances and angles of the calculated geometry for complexes **1–5**, as accessed by the geometry optimization, are presented in Table III. The optimized structures of the complexes **1** and **3** are shown in Figs. 1a and 1b, respectively.

TABLE III. Selected bond distances and bond angle values for complexes **1–5**, as obtained by the semi-empirical MO PM6 method in vacuum

PM6	<b>1</b>	<b>2</b>	<b>3</b>	<b>4</b>	<b>5</b>
Total energy, eV	−3579.16	−3861.72	−3628.15	−3665.11	−3964.50
$\Delta H_f / \text{kJ mol}^{-1}$ , vacuum implicit water model	−496.64	−727.48	−399.42	−350.89	−364.40
Distance N6–C16 (N12–C17), Å	1.331 (1.331)	1.333 (1.333)	1.338 (1.338)	1.331 (1.331)	1.331 (1.331)
Angle S18–Mo13–S20, °	82.152	87.400	87.432	87.321	87.334
Angle S19–Mo13–S21, °	148.494	148.60	148.545	148.453	148.502
Angle S19–Mo13–S18 (S21–Mo13–S20), °	68.642 (68.641)	68.788 (68.782)	68.698 (68.695)	68.705 (68.705)	68.713 (68.713)
Angle O15–Mo13–O14, °	107.508	107.531	107.672	107.493	107.476
Distance O15–Mo13 (O14–Mo13), Å	1.681 (1.681)	1.680 (1.680)	1.680 (1.680)	1.680 (1.680)	1.681 (1.681)
Distance S18–Mo13 (S20–Mo13), Å	2.635 (2.635)	2.636 (2.637)	2.636 (2.635)	2.638 (2.638)	2.639 (2.639)

TABLE III. Continued

PM6	1	2	3	4	5
Distance S19–Mo13 (S21–Mo13), Å	2.456 (2.456)	2.457 (2.456)	2.456 (2.455)	2.457 (2.457)	2.457 (2.457)
Distance C16–S19 (S18–C16), Å	1.742 (1.710)	1.740 (1.707)	1.739 (1.706)	1.740 (1.709)	1.741 (1.709)
Distance C17–S21 (C17–S20), Å	1.742 (1.710)	1.740 (1.707)	1.737 (1.706)	1.740 (1.709)	1.741 (1.709)
Angle O15–Mo13–S19 (O15–Mo13–S20), °	104.068 (160.266)	103.809 (160.562)	103.712 (160.548)	103.987 (160.386)	104.012 (160.381)
Angle O15–Mo13–S18 (O15–Mo13–S21), °	87.166 (97.432)	86.976 (94.671)	86.876 (94.769)	87.150 (94.569)	87.135 (94.530)
Angle O14–Mo13–S21 (O14–Mo13–S18), °	104.130 (160.250)	103.804 (160.566)	103.700 (160.528)	104.000 (160.394)	104.222 (160.378)
Angle O14–Mo13–S19 (O14–Mo13–S20), °	94.451 (87.125)	94.656 (86.956)	94.749 (86.871)	94.573 (87.133)	94.530 (87.142)
Angle S19–C16–S18 (S21–C17–S20), °	112.754 (112.764)	113.380 (113.380)	113.261 (113.255)	113.140 (113.142)	113.111 (113.112)

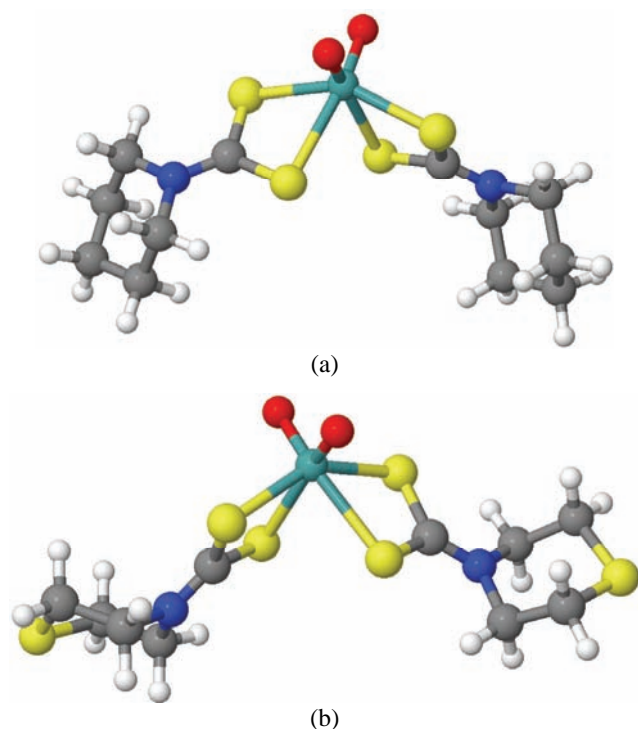


Fig. 1. Optimized geometry of the complexes obtained by the semi-empirical MO PM6 method:

a)  $[\text{MoO}_2(\text{Pipdte})_2]$  (1);  
 b)  $[\text{MoO}_2(\text{Timdte})_2]$  (3).

The non-hydrogen atoms numbering in Table III correspond to the labels as given in Scheme 1. The complexes **1–5** represent a deformed octahedral structure around the metal atom with the two oxygen atoms in the *cis*-position. The S–Mo–S



chelate angle of  $69^\circ$  is in agreement with X-ray crystal structures for this type of complexes.<sup>51,53</sup> Length difference between Mo13–S18 (Mo13–S20) and Mo13–S19 (Mo13–S21) is a consequence of the *trans* influence of the oxo-group.<sup>45</sup> The two Rdtc<sup>-</sup> ligands are oriented in the *cis*-position toward each other coordinated to metal ion *via* their deprotonated dithiocarbamato (CS<sub>2</sub><sup>-</sup>) groups, as presented in Figs. 1a and 1b for complexes **1** and **3**, respectively. The short N–C distance indicates a significant double bond character of these bonds.

In all the complexes, the heterocyclic parts of both ligands are in the chair conformation. The improper torsion angle in the heterocyclic part of the ligands, defined by the angle between the bonds C1–C2 and C5–C6 (C7–C8 and C11–C12) smaller than  $1^\circ$ , demonstrate an almost ideal chair conformation for the ligands in all the complexes. The planes of the cyclic part of the ligands, in the chair conformation, are oriented to each other at an angle of *ca.*  $180^\circ$ . The obtained results of molecular modeling demonstrate C<sub>2</sub> symmetry for all the complexes. Degree of deformation from an ideal octahedral structure is represented by the bond and torsion angles in the coordination sphere (Table III). The HOMO (highest occupied molecular orbital), HOMO-1 and HOMO-2 orbitals are located almost exclusively on the dioxo oxygen atoms and the dithiocarbamato sulfur atoms, as exemplified for complex **1** in Fig. 2, indicating involve-

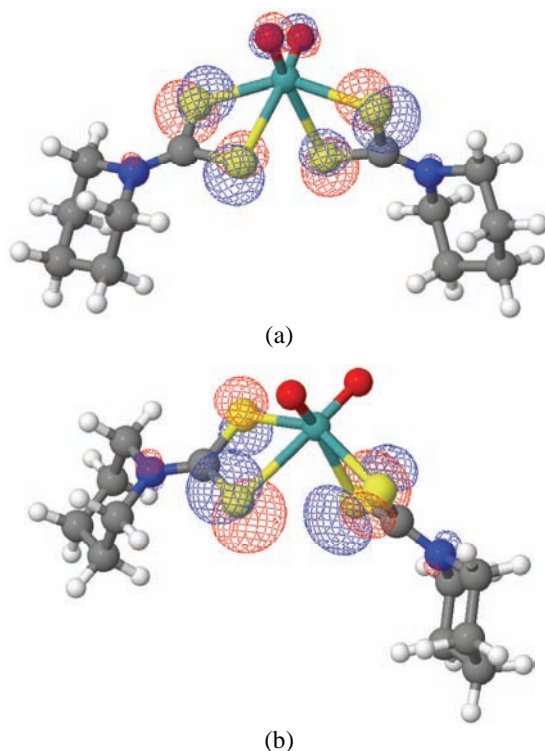


Fig. 2. a) HOMO ( $-8.31$  eV) and b) HOMO-1 ( $-8.38$  eV) of complex **1**.

ments of molybdenum  $d_{x^2-y^2}$  and  $d_{z^2}$  orbitals in the coordination. All the complexes appear to be somewhat more stable (have a more negative heat of formation) in the implicit water model than in vacuum, probably due to favorable electrostatic interactions of the heteroatoms (N, O, S), accessible to the solvent. Calculated structures of complexes **1** and **3** were superimposed on similar<sup>53</sup> or the same<sup>51</sup> experimentally obtained structures taken from the literature (Fig. S5 in the Supplementary material). For the superimposition, the coordination sphere ( $\text{MoO}_2=\text{S}_2\text{C}-$ ) and the heterocyclic N connected to dithiocarbamate moiety were used. The very good agreement should be noted. The calculated structure of complex **1** and the literature dioxomolybdenum di-(dithiocarbamate-*N*-pyrrolo) complex (CSD code 153544) superimpose their coordination spheres with a root-mean square deviation of 0.147. The calculated structure of complex **3** and the same experimentally obtained structures taken from literature superimpose their coordination spheres with a root-mean square deviation of 0.113. It should be noted that the symmetrically oriented thiomorpholino part of the ligands for complex **3**, as obtained by semi-empirical calculations, appears somewhat more stable both in solution and in vacuum than the asymmetrically oriented ones found in the crystal structure.

#### *Suggested structure*

The important features of the IR spectra provide a consistent picture that the  $\text{Rdtc}^-$  ligands are bound through the both sulfur atoms to the molybdenum atom, as it can also be seen from the chemical environments of the  $\text{CS}_2$  moieties in the NMR spectra. This bidentate  $S,S'$  structure is again the most favorable in comparison with a monodentate one. The geometry of the  $\text{MoO}_2\text{S}_4$  core is a distorted octahedron (Fig. 1) with the two terminal oxo ligands lying invariably in a *cis*-position to each other, usual for dioxomolybdenum(VI) complexes,<sup>51–53</sup> while the two  $\text{Rdtc}^-$  ligands complete the distorted octahedral coordination. Based on the above calculation (Table III), the influence of the variation of the heteroatom in position 4 of the piperidine moiety on the coordination sphere can be straightforwardly elucidated.

#### *Antimicrobial activity*

The results of the obtained antimicrobial activities of  $[\text{MoO}_2(\text{acac})_2]$ , the five  $\text{Rdtc}^-$  ligands, complexes **1–5**, standard antibiotics and nystatin are presented in Tables IV and V. Generally, the complexes were more potent than the corresponding ligands and  $[\text{MoO}_2(\text{acac})_2]$ . Obviously, the introduction of a heteroatom in position 4 of the piperidino moiety makes the complexes significantly more potent in respect to the corresponding ligands. A higher potency of the ligand compared to the complexes was only observed in the data of complex **1**, for some of the tested microbial strains (Table IV).

TABLE IV. Minimal inhibitory concentrations (MIC) of the tested compounds

Microorganism	[MoO <sub>2</sub> (acac) <sub>2</sub> ]	Complexes/corresponding ligand				
		1/L	2/L	3/L	4/L	5/L
<i>S. aureus</i> ATCC 25923 <sup>a</sup>	3.81	5.56/6.21	5.53/22.8	2.58/45.6	2.78/11.4	10.5/10.7
<i>S. epidermidis</i> ATCC 12228	7.62	2.79/6.21	2.76/22.8	2.58/22.8	1.39/11.4	2.61/10.7
<i>M. luteus</i> ATCC 9341	13.81	5.56/1.24	5.53/22.8	2.58/22.8	2.78/11.4	2.61/5.38
<i>M. flavus</i> ATCC 10240	3.81	5.56/1.24	2.76/22.8	2.58/45.6	2.78/11.4	2.61/5.38
<i>E. faecalis</i> ATCC 29212	7.62	5.56/49.6	2.76/45.6	2.58/45.6	2.78/11.4	2.61/10.7
<i>B. subtilis</i> ATCC 6633	7.62	5.56/1.24	2.76/22.8	2.58/22.8	2.78/11.4	2.61/10.7
<i>E. coli</i> ATCC 25922	7.62	5.56/6.21	2.76/45.6	2.58/45.6	2.78/11.4	2.61/10.7
<i>K. pneumoniae</i> NCIMB 9111 <sup>b</sup>	7.62	5.56/6.21	2.76/45.6	2.58/45.6	2.78/11.4	2.61/10.7
<i>P. aeruginosa</i> ATCC 27853	7.62	5.56/49.6	5.53/45.6	5.16/45.6	5.55/22.9	2.61/10.7
<i>C. albicans</i> ATCC 10259	7.62	2.79/2.48	11.2/11.38	2.58/22.8	2.78/5.72	2.61/5.38
<i>C. albicans</i> ATCC 24433	7.62	2.79/2.48	11.2/5.69	2.58/22.8	2.78/5.72	2.61/5.38

<sup>a</sup>American Type Culture Collection (<http://www.atcc.org/>); <sup>b</sup>National Collections of Industrial Food and Marine Bacteria: NCIMB Ltd, UK

TABLE V. Minimal inhibitory concentrations (MIC) of the standard antibiotics against the tested microbial strains (n.t. – not tested)

Microorganism	Amikacin	Ampicillin	Vancomycin	Nystatin
<i>S. aureus</i> ATCC 25923	3.42	2.86	1.52	n.t.
<i>S. epidermidis</i> ATCC 12228	n.t.	n.t.	1.38	n.t.
<i>M. luteus</i> ATCC 9341	n.t.	10.3	n.t.	n.t.
<i>M. flavus</i> ATCC 10240	n.t.	12.0	n.t.	n.t.
<i>E. faecalis</i> ATCC 29212	4.09	n.t.	n.t.	n.t.
<i>E. coli</i> ATCC 25922	14.7	12.6	n.t.	n.t.
<i>K. pneumoniae</i> NCIMB 9111	10.9	n.t.	n.t.	n.t.
<i>P. aeruginosa</i> ATCC 27853	4.78	n.t.	n.t.	n.t.
<i>C. albicans</i> ATCC 10259	n.t.	n.t.	n.t.	4.1
<i>C. albicans</i> ATCC 24433	n.t.	n.t.	n.t.	6.69

It should be noted that all the complexes were active against *S. epidermidis*, as well as against *P. aeruginosa*, which is one of the most resistant human pathogen.

## CONCLUSIONS

The present study demonstrates simple synthetic routes to five new dioxomolybdenum(VI) complexes with heterocyclic dithiocarbamates. The employed spectroscopic techniques suggest that the coordination in all  $[\text{MoO}_2(\text{Rdte})_2]$  complexes yielded an octahedral geometry through both sulfur donating atoms, the NCSS group coordinating the metal center in a bidentate symmetrical mode. The geometries of **1–5**, obtained on semi-empirical MO PM6 levels are in good agreement with similar complexes for which X-ray structure data can be found in the literature. The dioxomolybdenumdithiocarbamates were capable of inhibiting bacterial growth to a certain degree.

## SUPPLEMENTARY MATERIAL

IR,  $^1\text{H}$ - and  $^{13}\text{C}$ -NMR spectra of synthesized compounds are available electronically from <http://www.shd.org.rs/JSCS/>, or from the corresponding author on request.

*Acknowledgments.* This research was supported by the Ministry of Education and Science of the Republic Serbia (No. 172014).

## ИЗВОД

СПЕКТРОСКОПСКА СВОЈСТВА И АНТИМИКРОБНА АКТИВНОСТ ДИОКСОМОЛИБДЕН(VI) КОМПЛЕКСА СА ХЕТЕРОЦИКЛИЧНИМ  $S,S'$ -ЛИГАНДИМА

СОФИЈА П. СОВИЉ<sup>1</sup>, ДРАГАНА МИТИЋ<sup>1</sup>, БРАНКО Ј. ДРАКУЛИЋ<sup>2</sup> И МАРИНА МИЛЕНКОВИЋ<sup>3</sup>

<sup>1</sup>Хемијски факултет Универзитета у Београду, б. бр. 118, 11158 Београд, <sup>2</sup>Институт за хемију, технологију и металургију – Центар за хемију, Њеђошева 12, 11001 Београд и <sup>3</sup>Фармацеутички факултет, Универзитета у Београду, Војводе Сіеје 450, 11000 Београд

Синтетисано је пет нових диоксомолибден(VI) комплекса, опште формуле  $[\text{MoO}_2(\text{Rdte})_2]$ , са  $\text{Rdte}^-$  лигандима: пиперидин- ( $\text{Pipdte}$ ), 4-морфолин- ( $\text{Morphdte}$ ), 4-тиоморфолин- ( $\text{Timdte}$ ), пиперазин- ( $\text{Pzdte}$ ) и  $N$ -метилпиперазин- ( $N\text{-Merpzdte}$ ) дитиокарбаматима. Комплекси су окарактерисани елементалном анализом, IR и NMR спектроскопијом као и мерењем моларне проводљивости. Претпостављена геометрија свих комплекса је октаедарска.  $\text{Rdte}^-$  лиганди су бидентатно координовани преко оба атома сумпора за атом молибдена. Присуство различитих хетероатома утиче на промену положаја  $\nu(\text{C}=\text{H})$  и  $\nu(\text{C}=\text{S})$  вибрација, чији опада следећим редом лиганда:  $\text{Pipdte} > N\text{-Merpzdte} > \text{Morphdt} > \text{Pzdte} > \text{Timdte}$ . На основу спектралних података, структуре свих комплекса су оптимизоване на семиемпиријском молекулско-орбиталном нивоу употребом PM6 метода. Антимикробна активност испитивана је на једанаест различитих патогена. Уочено је да комплекси који имају хетероатом у положају 4 пиперидинског прстена испољавају значајно већу јачину антимикробног дејства према бактеријама, у поређењу са одговарајућим лигандима.

(Примљено 28. марта, ревидирано 26. августа 2011)

## REFERENCES

1. R. R. Mendel, F. Bittner, *Biochim. Biophys. Acta, Mol. Cell Res.* **1763** (2006) 621
2. A. Sigel, H. Sigel, Eds., *Metal Ions in Biological Systems 39, Molybdenum and Tungsten: Their Roles in Biological Processes*, Marcel Dekker, New York, 2002
3. J. Davis, *Science* **264** (1994) 375

4. R. F. Service, *Science* **270** (1995) 724
5. C. D. Brondino, M. G. Rivas, M. J. Romao, J. G. Jose, I. Moura, *Acc. Chem. Res.* **39** (2006) 788
6. G. Schwarz, R. R. Mendel, *Annu. Rev. Plant Biol.* **57** (2006) 623
7. J. H. Enemark, A. V. Astashkin, A. M. Raitsimring, *Dalton Trans.* **29** (2006) 3501
8. P. Nag, R. Bohra, R. C. Mehrotra, R. Ratnani, *Synth. React. Inorg. Met.-Org. Chem.* **32** (2002) 1549
9. D. Coucouvanis, *Prog. Inorg. Chem.* **26** (1989) 301
10. S. P. Sovilj, G. Vučković, K. Babić, S. Macura, N. Juranić, *J. Coord. Chem.* **41** (1997) 19
11. S. P. Sovilj, K. Babić-Samardžija, *Synth. React. Inorg. Met.-Org. Chem.* **29** (1999) 1655
12. L. I. Victoriano, *Coord. Chem. Rev.* **196** (2000) 383 (and references cited therein)
13. S. P. Sovilj, N. Avramović, D. Poletić, D. Djoković, *Bull. Chem. Technol. Maced.* **19** (2000) 139
14. S. P. Sovilj, N. Avramović, N. Katsaros, *Transition Met. Chem.* **29** (2004) 737
15. K. B. Pandeya, B. B. Kaul, *Synth. React. Inorg. Met.-Org. Chem.* **12** (1982) 259
16. S. O. Pinheiro, J. R. de Sousa, M. O. Santiago, I. M. Carvalho, Y. Hao, W. Perez-Segarra, Q. Shi, A. Wei, *J. Am. Chem. Soc.* **127** (2005) 7328
17. J. D. E. T. Wilton-Ely, D. Solanki, G. Hogarth, *Eur. J. Inorg. Chem.* (2005) 4027
18. A. L. R. Silva, A. A. Batista, E. E. Castellano, J. Ellena, I. S. Moreira, I. C. N. Diogenes, *Inorg. Chim. Acta* **359** (2006) 391
19. S. P. Sovilj, D. Mitić, V. M. Leovac, *Asian J. Chem.* **15** (2003) 165
20. C. Bolzati, M. C. Ceccato, S. Agostini, F. Refosco, Y. Yamamichi, S. Tokunaga, D. Carta, N. Salvarese, D. Bernardini, G. Bandoli, *Bioconjugate Chem.* **21** (2010) 928
21. H. Li, C. S. Lai, J. Wu, P. C. Ho, D. de Vos, E. R. T. Tiekink, *J. Inorg. Biochem.* **101** (2007) 809
22. Z. A. Kaplancikli, G. Turan-Zitouni, G. Revial, G. Iscan, *Phosphorus, Sulfur Silicon Relat. Elem.* **179** (2004) 1449
23. N. K. Kaushik, B. Bushan, A. K. Sharma, *Transition Met. Chem.* **9** (1984) 250
24. N. Katsaros, M. Katsaroua, S. P. Sovilj, K. Babić-Samardžija, D. M. Mitić, *Bioinorg. Chem. App.* **2** (2004) 193
25. N. Hackerman, D. D. Justice, E. McCafferty, *Corrosion* **31** (1975) 240
26. V. M. Jovanović, K. Babić-Samardžija, S. P. Sovilj, *Electroanalysis* **13** (2001) 1129
27. V. M. Jovanović, K. Babić-Samardžija, S. P. Sovilj, *J. Serb. Chem. Soc.* **70** (2005) 51
28. S. P. Sovilj, B. J. Drakulić, D. Lj. Stojić, N. Katsaros, *Mater. Sci. Forum* **518** (2006) 411
29. E. Farkas, H. Csoka, G. Bell, D. A. Brown, L. P. Cuffe, N. J. Fitzpatrick, W. K. Glass, *J. Chem. Soc., Dalton Trans.* **16** (1999) 2789
30. A. C. Stergiou, S. Bladenopoulou, C. Tsiamis, *Inorg. Chim. Acta* **217** (1994) 61
31. B. B. Kaul, J. H. Enemark, S. L. Merbs, J. T. Spence, *J. Am. Chem. Soc.* **107** (1985) 2885
32. K. Babić-Samardžija, S. P. Sovilj, N. Katsaros, *J. Molec. Struct.* **694** (2004) 165
33. M. M. Jones, *J. Am. Chem. Soc.* **81** (1959) 3188
34. a) J. J. P. Stewart, *J. Comput.-Aided Mol. Des.* **4** (1990) 1; b) J. J. P. Stewart, MOPAC2009, Stewart Computational Chemistry, Colorado Springs, CO, 2009, <http://OpenMOPAC.net> (accessed on 17/03/2011)
35. J. J. P. Stewart, *J. Mol. Model.* **13** (2007) 1173
36. A. Klamt, G. Schüümann, *J. Chem. Soc., Perkin Trans. 2* (1993) 799
37. K. Wolinski, J. F. Hilton, P. Pulay, *J. Am. Chem. Soc.* **112** (1990) 8251

38. S. Miertus, E. Scrocco, J. Tomasi, *Chem. Phys.* **55** (1981) 117
39. *GAUSSIAN 03, Revision C.02*, Gaussian, Inc., Pittsburgh, PA, 2003
40. A. Pedretti, L. Villa, G. Vistoli, *J. Comput.-Aided Mol. Des.* **18** (2004) 167
41. *Jmol: an open-source Java Viewer for Chemical Structures in 3D*, *Jmol v.11.2.1*, <http://www.jmol.org/> (accessed on 17/03/2011)
42. Clinical and Laboratory Standards Institute (CLSI), *Performance Standards for Antimicrobial Susceptibility Testing: 15<sup>th</sup> Informational Supplement*, CLSI Document M100-S15, Wayne, PA, USA, 2005
43. W. J. Geary, *Coord. Chem. Rev.* **7** (1971) 81
44. R. J. H. Clark, T. J. Dines, M. J. Wolf, *J. Chem. Soc., Faraday Trans. 2* **78** (1982) 679
45. H. O. Desseyn, A. C. Fabretti, F. Forghieri, C. Preti, *Spectrochim. Acta, Part A* **41** (1985) 1105
46. A. C. Fabretti, F. Forghieri, A. Giusti, C. Preti, G. Tosi, *Inorg. Chim. Acta* **85** (1984) 127
47. L. J. Willis, T. M. Loehr, K. F. Miller, A. E. Bruce, E. I. Stiefl, *Inorg. Chem.* **25** (1986) 4289
48. F. A. Cotton, G. Wilkinson, C. A. Murillo, M. Bochmann, *Advanced Inorganic Chemistry*, 6<sup>th</sup> ed., Wiley, New York, 1999, Chap. 18, p. 944
49. K. Nakamoto, *Infrared and Raman Spectra of Inorganic and Coordination Compounds*, 5<sup>th</sup> ed., Wiley, New York, 1988, p. 82
50. G. Faraglia, S. Sitran, *Inorg. Chim. Acta* **176** (1990) 67
51. K. Unoura, A. Yamazaky, A. Nagasawa, H. Itoh, H. Kudo, Y. Fukuda, *Inorg. Chim. Acta* **269** (1998) 260
52. L. Stelzig, S. Kotte, B. Krebs, *J. Chem. Soc., Dalton Trans.* **17** (1998) 2921
53. H. Teruel, Y. C. Gorin, L. R. Falvello, *Inorg. Chim. Acta* **316** (2001) 1.